Spectroscopic characterization of manganese-doped alkaline earth lead zinc phosphate glasses

S SREEHARI SASTRY[1,*] **and B RUPA VENKATESWARA RAO**[1,2]

[1]Department of Physics, Acharya Nagarjuna University, Nagarjunanagar 522 510, India
[2]Department of Physics, V.R. Siddhartha Engineering College, Vijayawada 520 007, India

Abstract.   Alkaline earth lead zinc phosphate glasses doped with Mn(II) are characterized by spectroscopic techniques like X-ray diffraction (XRD), UV–visible, differential scanning calorimetry (DSC), electron paramagnetic resonance (EPR), Fourier transform infrared (FTIR) and Raman. Optical absorption spectrum exhibits four bands which are characteristic of Mn(II) in distorted octahedral site symmetry. The crystal field parameter Dq and Racah interelectronic-repulsion parameters *B* and *C* have been evaluated. All investigated samples exhibit EPR signals which are characteristic to the Mn^{2+} ions. The shapes of spectra are also changed with varying alkaline earth ions content. FTIR spectra show specific vibrations of phosphate units. The characteristic Raman bands of these glasses due to stretching and bending vibrations were identified and analysed by varying alkaline earth content. The intensity and frequency variations for the characteristic phosphate group vibrations have been correlated with the changes of the structural units present in these glasses. Depolymerization of the phosphate chains in all the glasses is observed with replacement of alkaline earth content by spectroscopic studies. This leads to a strong decrease of the average chain length and a small decrease of the average P–O–P bridging angle with replacement of alkaline earth content.

Keywords.   Glasses; UV–vis; DSC; EPR; FTIR; Raman spectral studies; Racah parameters.

1. Introduction

Recent technological applications have generated more importance in the studies of different types of glasses owing to their structural properties.[1,2] One of them is phosphate glass, which owing to their hygroscopic nature and volatility was not considered to have industrial and technological applications. But in the recent developments of novel compositions of superior physical and chemical properties such as high thermal expansion coefficients,[3] high ultra-violet and far infrared transmission,[4] low melting and softening temperatures, make these glasses potential candidates for many technological applications, such as medical use and sealing materials.[5]

The interest in glasses containing transition metal ions has grown[6] because these glasses have properties of technological importance. Among all the transition metal ions, manganese (^{55}Mn) have been recurrently used as paramagnetic probes to investigate the structure and properties of vitreous systems, as manganese ions have a strong demeanor on the magnetic and optical properties of the glass. In glass matrices manganese ions exist in different valence states occupying tetrahedral or octahedral sites in glass network. The content of manganese in various environments and valence states in the glasses depends on the quantitative properties of modifiers and glass formers, size of the ions in the glass structure, their field strength, mobility of the modifier cation, etc.[7] Hence, connection between state and position of manganese ion and electrical properties of glass containing mobile ions like $Mg^{2+}/Ca^{2+}/Sr^{2+}/Ba^{2+}$ is expected to be interesting. Spectroscopic techniques made to obtain information on some of structural and dynamic phenomenon of a material; and to identify the site symmetry around the transition metal ions in glasses.[8] The aim of present investigation is to study the nature of site symmetry of Mn^{2+} in alkaline earth lead zinc phosphate glasses along with compositional variation of alkaline earth content.

2. Experimental

The glasses under study were prepared from chemically pure AnalaR grade reagents such as P_2O_5, Pb_3O_4, ZnO, 0.1 mol% of MnO and MgO, CaO, SrO, BaO were added as an intermediate compound to each glass composition. The weighed batches were melted in porcelain crucibles at 1100°C for 1 h. The melts were rotated several times and the homogenized melts were poured in slightly warmed brass molds of the required dimensions. The prepared samples were immediately transferred to an annealing furnace regulated at 300°C for about 5 h to relieve mechanical strains and cracking of the glass samples. The compositions of the glass samples employed in the study are given in table 1.

*Author for correspondence (sreeharisastry@yahoo.com)

Table 1. Glass compositions (mol%).

| Samples	Composition (mol%)
TG4A	$59.9P_2O_5–10Pb_3O_4–10ZnO–20MgO–0.1MnO$
TG4B	$59.9P_2O_5–10Pb_3O_4–10ZnO–20CaO–0.1MnO$
TG4C	$5939P_2O_5–10Pb_3O_4–10ZnO–20Sro–0.1MnO$
TG4D	$59.9P_2O_5–10Pb_3O_4–10ZnO–20BaO–0.1MnO$

The amorphous nature of the glass is investigated through the X-ray diffraction (XRD) patterns recorded on powder samples at room temperature using Philips X-ray generator (Model PW1170) with CuK$_\alpha$ radiation (λ=1.5418 Å) in the 2θ ranges from $10°$ to $70°$, with a step size of $2°$ per minute. The differential scanning calorimetry (DSC) measurements were performed using Netzsch DSC 204 instrument. A small amount of material about 5–10 mg was taken in the aluminium pan of the DSC set-up and scanned at a heating rate of $10°C$ min^{-1}. The optical absorption spectra of these glasses were recorded to a resolution of 0.1 nm at room temperature in the spectral wavelength range covering from 200 to 900 nm using JASCO model V-670 UV–vis–NIR spectrophotometer. Electron paramagnetic resonance (EPR) spectra were made at room temperature through BRUKER-ER073 series of EPR spectrometer which operates in the X-band frequency (9.4 GHz) at 100 kHz field modulation. The magnetic field was scanned from 0 to 800 mT and the microwave power used was 1 mW. The infrared spectra of alkali earth lead zinc phosphate glasses were recorded on SHIMADZU 8201 PC FTIR spectrophotometer in the range 4000–400 cm^{-1} using KBr pellets. With Raman spectrometer (Lab RAM HR-800-HORIBAJOBINYVON) equipped with argon ion laser 514.25 nm, which eliminates the problem of sample fluorescence and photo-decomposition. The glass samples were subjected for the Raman spectra in the range 200–3500 cm^{-1} with 1.0 mW laser power. The formulae and process applied here to resolve the physical properties in the study were put to test in earlier works of authors.[9,10]

3. Results and discussion

The chemical composition of glass samples which are shown in table 1 are prepared for the present study. The change in atomic geometrical configuration, co-ordination number, cross-link density and the dimensions of the interstitial space in the glass network decides the density. Hence, the density is a tool in revealing the degree of change in the structure with any glass composition.[11] The increase in density for the glass system reveals the change in the structure of the glass with replacement of alkaline earth content. The density of a glass is found to be very sensitive to the ionic size and atomic weight.[12] The data in table 2 indicate that average molecular weight increases from TG4A to TG4D glass which influences density, refractive index and other physical properties. The density and refractive index of TG4D glass is more, this can be due to the addition of Ba^{2+} provides ionic

Table 2. Physical properties of Mn^{2+}-doped alkaline earth lead zinc phosphate glasses.

Physical property	TG4A	TG4B	TG4C	TG4D
Refractive index (nd) at 589.3 nm	1.6405	1.6450	1.6550	1.6605
Density, d (g cm^{-3})	3.6275	3.6309	3.8710	3.9324
Average molecular weight, M (g)	169.852	173.007	182.515	192.457
Mean atomic volume (g cm^{-3} per atom)	8.5210	8.5804	8.6712	8.9065
Molar volume, V_m (cm^3)	46.8234	47.6485	47.1493	48.9431
Optical basicity Λ_{th}	0.4132	0.4441	0.4451	0.4525
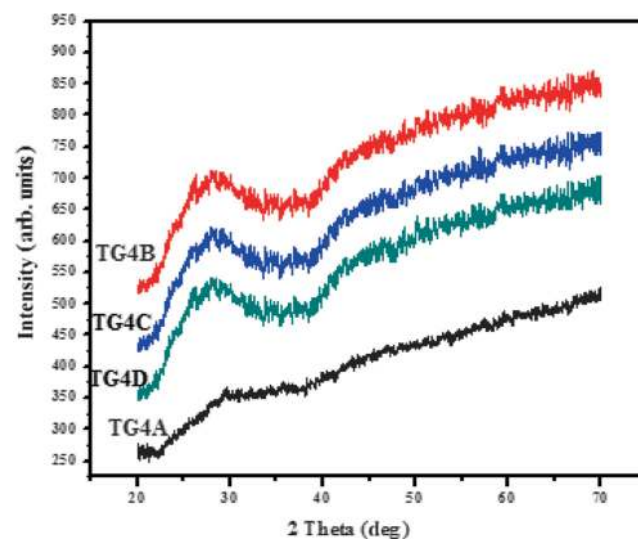
Figure 1. XRD spectra of Mn^{2+}-doped alkaline earth lead zinc phosphate glasses.

cross-linking between non-bridging oxygen's and increases the bond strengthof this cross-link is expected to improve chemical durability. The increase in refractive index is attributed to the generation of non-bridging oxygen (NBO). Molar volume is gradually increased with successive substitution of MgO/CaO/SrO/BaO, suggests increased free space within glass structure and changes in the structure.[13,14] Basicity parameter slightly increases from glass TG4A to TG4D. High optical basicity means high electron donor ability o oxide ions to the cations. The optical basicity can be used to classify the covalent/ionic character of the glasses since an increasing Λ_{th} indicates decreasing covalence.[15] Deviation in properties also infers that environment around manganese ions is different in different glasses which are due to replacement of alkali earth oxide effects.

Figure 1 shows the XRD patterns of Mn^{2+}-doped alkaline earth lead zinc phosphate glass systems. No significant crystalline peaks recorded in the patterns, it is confirmed here the amorphous nature of glass samples.

DSC monitors heat effects allied with the phase transitions and chemical reactions as a role of temperature. DSC

thermograms of present glass system are shown in figure 2. All the glasses exhibited an endothermic change due to the glass transition temperature T_g occurred between 360 and 380°C. For higher temperatures all the sampled glasses exhibited an exothermic change due to crystallization temperature T_c reported between 400 and 425°C. The values of T_g, T_c and T_c–T_g are presented in table 3. The T_c–T_g values present the information on the stability of the glass against devitrification.[16]

The network modifiers directly influence the T_g because glass transition involves modification of chemical bonds between the glass former and glass modifiers. Generally, the T_g of oxide glasses increase with the bond strength, cross-link density and closeness of packing.[17] The introduction of a glass modifier such as RO into the oxide glass modifies the oxide network.[18–20]

On the basis of the above literature reports, the results obtained in the present study can be interpreted as follows. The increase in glass transition temperature values reflects an increase of cross-link strength of glass network as Mg^{2+} or Ca^{2+} or Sr^{2+} or Ba^{2+} ions are introduced in the phosphate glass. The increased cross-linking appears to be responsible for better chemical durability of the doped glasses. Thus glass with maximum T_g value is the most durable one out of all other glasses studied.

The absorption spectrum shows $Mn^{2+}(d^5)$ can occur in glasses both in tetrahedral and octahedral environments. The UV–visible absorption spectra of Mn^{2+}-doped alkaline earth lead zinc phosphate glass samples is shown in figure 3. It is observed that, four bands nearly at around 370, 406, 450 and 530 are assigned to the transitions $^6A_{1g}(S) \rightarrow {}^4T_{1g}(G)$, $^6A_{1g}(S) \rightarrow {}^4T_{2g}(G)$, $^6A_{1g}(S) \rightarrow {}^4A_{1g}(G) + {}^4E_g(G)$ and $^6A_{1g}(S) \rightarrow {}^4T_{2g}(D)$, characteristic of Mn^{2+} ions in octahedral symmetry[21–23] and the band positions are presented in table 4. The analysis shows that manganese ions exist mainly in Mn^{2+} state, occupy tetrahedral positions. Optical spectra have been analysed in the framework of crystal field theory.[24] The excited quartet states ^4G, ^4P, ^4D and ^4F of Mn^{2+} ions in octahedral crystal field are located above the ground ^6S state
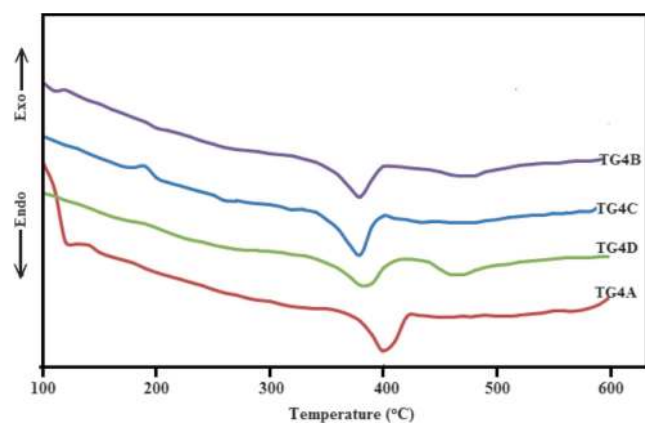
and trigonal crystal field splits four levels into ten sublevels. Therefore, all the transitions from the ground sextet ^6S to the excited levels are spin-forbidden, intensity of optical absorption lines of Mn^{2+} are weak and in addition, Mn^{2+} ion had a $3d^5$ configuration. The absorption band at around 450 nm was asymmetric, indicating that the octahedral ligand field had suffered a tetrahedral deformation by the Jahn–Teller effect. The ligand field bands are sharp, when the energy expressions for the transition are independent of Dq whereas the bands are broad when they depend on Dq. The crystal-field parameter Dq and the inter-electronic repulsion parameters B and C have been evaluated by energy matrices[25] for the d^5 configuration. In the analysis of the optical spectrum, Trees' correction parameter[26] 'α'= 76 cm^{-1} has also been incorporated to obtain a good fit between the observed and calculated values. The crystal fields and inter-electronic repulsion parameters are given in table 5. The values of Dq/B and C/B represent structural distortion and which is observed to be high in BaO-based glass. The obtained B values decreases gradually from TG4A glass to TG4D glass, such decrease indicates an increase in average distance of Mn–O in the glass matrix.[27]

The absorption edge study in the UV region is a useful method to understand the optical transition and electronic band structure in glasses. The principle of this technique is that a photon with energy greater than the band gap energy will be absorbed. The photoconductivity spectral response of such materials rises sharply at about the same frequency as the optical absorption edge.[28] The absorption edge, at low energy, normally follows the Urbach rule.[29] Such an edge can occur in glassy materials from inter-band transitions relating the tails of localized states, the density of which falls off exponentially with energy in the band gap.[30] The absorption coefficient $\alpha(v)$ for direct and indirect optical transitions is given by following equation:[31]

$$\alpha(v) = \frac{a_0 \left[hv - E_{opt} \right]^n}{hv}, \tag{1}$$

where exponent $n = 1/2$ for an allowed direct transition, while $n = 2$ for an allowed indirect transition, α_0 is a constant related to the extent of the band tailing and E_{opt} the optical band gap energy. The absorption coefficient, $\alpha(v)$, can be determined near the absorption edge of different photon energies for all glass samples. The values of optical band ga energy (E_{opt}) can be determined from the plot of $(\alpha hv)^{1/2}$

Figure 2. DSC pattern of Mn^{2+}-doped alkaline earth lead zinc phosphate glasses.

Table 3. Data on DSC traces of of Mn^{2+}-doped alkaline earth lead zinc phosphate glasses.

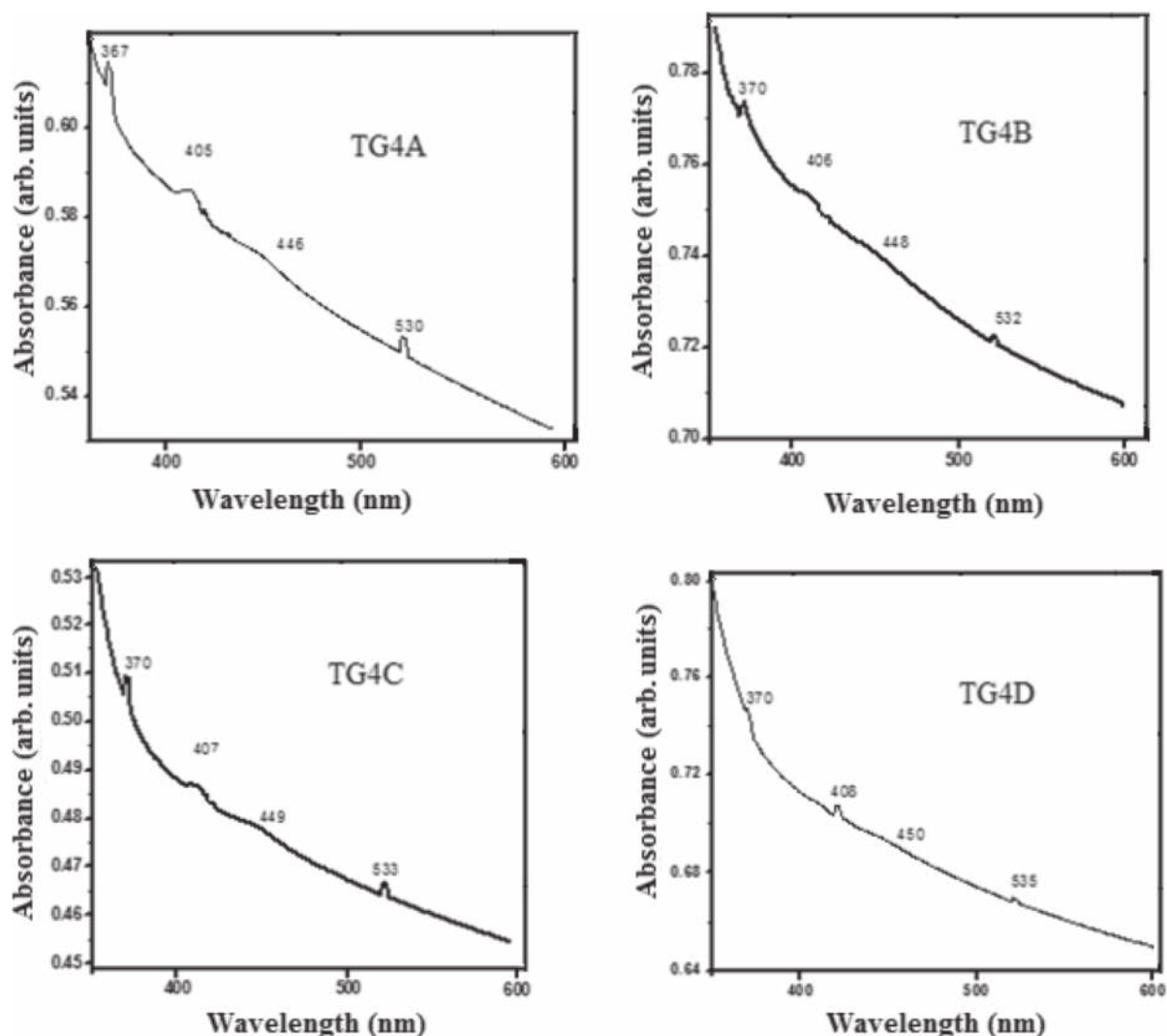| Sample	T_g (°C)	T_c (°C)	T_c–T_g (°C)
TG4A	379	422	43
TG4B	365	406	41
TG4C	362	401	39
TG4D	359	423	64

Figure 3. Optical absorption spectra of Mn^{2+}-doped alkaline earth lead zinc phosphate glasses.

vs. photon energy ($h\nu$) (Tauc's plot), for allowed indirect transitions.

Figure 4 shows Tauc's plots of Mn^{2+}-doped alkaline earth lead zinc phosphate glasses. Optical band gap (E_{opt}) and Urbach energy (ΔE) values are presented in table 6. Urbach energy decreases with replacement of alkaline earth, shows the structural disorder of the system. Smaller is the value of Urbach energy, greater is the structural stability of the glass system. It is observed that BaO-based glass (TG4D) have low value of structural disorder, which indicates the strong structural stability. The band gap energy calculations indicate that the glass systems are direct semiconductors.

The EPR spectra of Mn^{2+} are analysed using the spin-Hamiltonian of the form

$$H = g\beta BS + SAI + SDS, \qquad (2)$$

where g is the isotropic factor, β the Bohr magneton, B the external magnetic field, S the vector operator of the electron spin momentum and A the hyperfine interaction parameter,

I the vector operator of nuclear spin momentum and D the zero field splitting parameter.

EPR spectra of Mn^{2+} in a series of glasses have shown that the spectra have been characterized by an intense resonance signal at around $g = 2.0$ with six line hyperfine pattern, an absorption around $g = 4.3$ which is a characteristic of Mn^{2+} ions with a nuclear spin $I = 5/2$.[32] The ^{55}Mn hyperfine structure has two substantial benefits. (a) It commonly allows explicit assignments of positions of complex resonance lines to manganese and (b) the magnitude of hyperfine splitting constant provides a measure of bonding between Mn^{2+} ions and its neighbouring ligands.[33] In d^5 transition metal ions, it is well-known that axial distortion of octahedral symmetry gives rise to three Kramer's doublets $|\pm 5/2\rangle$, $|\pm 3/2\rangle$ and $|\pm 1/2\rangle$.[34] As the crystal field splitting is normally greater than the Zeeman field, the resonances observed are due to transitions in the Zeeman field split Kramer's doublets.

Recorded EPR spectra show resonance line due to Mn^{2+} ($3d^5, {}^6S_{5/2}$) paramagnetic ions for all glasses. The structure of

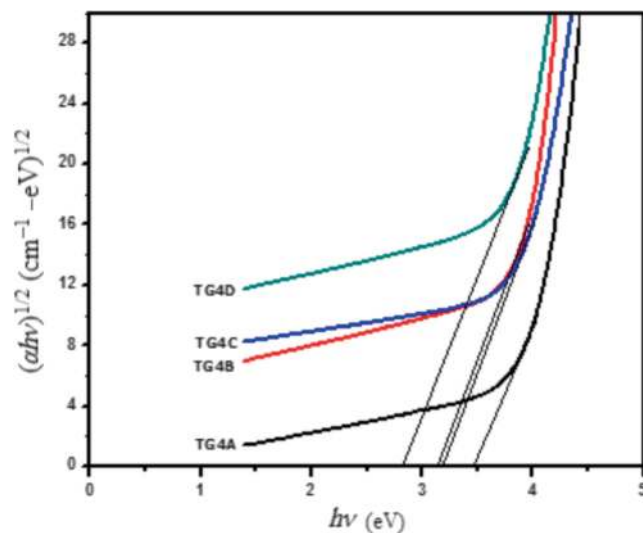**Table 4.** Optical absorption band positions of Mn^{2+}-doped alkaline earth lead zinc phosphate glasses.

Sample	Transitions	Wavelength (nm)	Wavenumber (cm^{-1}) Observed	Calculated
TG4A	$^6A_{1g}(S) \rightarrow {}^4T_{1g}(G)$	530	18,867	18,715
	$^6A_{1g}(S) \rightarrow {}^4T_{2g}(G)$	446	22,421	22,462
	$^6A_{1g}(S) \rightarrow {}^4A_{1g}(G) + {}^4E_g(G)$	405	24,691	24,742
	$^6A_{1g}(S) \rightarrow {}^4T_{2g}(D)$	368	27,173	27,240
TG4B	$^6A_{1g}(S) \rightarrow {}^4T_{1g}(G)$	532	18,796	18,634
	$^6A_{1g}(S) \rightarrow {}^4T_{2g}(G)$	448	22,321	22,347
	$^6A_{1g}(S) \rightarrow {}^4A_{1g}(G) + {}^4E_g(G)$	406	24,630	24,652
	$^6A_{1g}(S) \rightarrow {}^4T_{2g}(D)$	370	27,027	27,099
TG4C	$^6A_{1g}(S) \rightarrow {}^4T_{1g}(G)$	533	18,761	18,624
	$^6A_{1g}(S) \rightarrow {}^4T_{2g}(G)$	449	22,271	22,335
	$^6A_{1g}(S) \rightarrow {}^4A_{1g}(G) + {}^4E_g(G)$	407	24,570	24,642
	$^6A_{1g}(S) \rightarrow {}^4T_{2g}(D)$	370	27,027	27,083
TG4D	$^6A_{1g}(S) \rightarrow {}^4T_{1g}(G)$	535	18,691	18,597
	$^6A_{1g}(S) \rightarrow {}^4T_{2g}(G)$	450	22,222	22,296
	$^6A_{1g}(S) \rightarrow {}^4A_{1g}(G) + {}^4E_g(G)$	408	24,509	24,612
	$^6A_{1g}(S) \rightarrow {}^4T_{2g}(D)$	370	27,027	27,036

Table 5. Crystal fields and inter-electronic repulsion parameters of Mn^{2+}-doped alkaline earth lead zinc phosphate glasses.

Sample	Dq (cm^{-1})	B (cm^{-1})	C (cm^{-1})	α (cm^{-1})
TG4A	780	725	3200	76
TG4B	780	716	3200	76
TG4C	780	715	3200	76
TG4D	780	712	3200	76

Figure 4. Tauc's plots of Mn^{2+}-doped alkaline earth lead zinc phosphate glasses.

the spectra strongly depends on manganese content of samples. The EPR spectra are presented in figure 5. EPR spectra observed in alkaline earth lead zinc phosphate glass matrix consist of a well-resolved sextet centred at $g = 2.0$ with a broad background signal underneath the sextet and very well absorption centred at $g = 4.3$, which is characteristic for isolated Mn^{2+} ions in rhombic distorted octahedral environment, as shown in figure 5.

The $g = 2.0$ resonance line is known to arise from central $M_s = |-1/2\rangle \rightarrow |+1/2\rangle$ transition where M_s is the effective spin component. The six-line multiplet results from hyperfine interaction of electron spin with ^{55}Mn nucleus ($I = 5/2$). This isotropic signal at $g = 2.0$ is due to Mn^{2+} ions in an environment close to octahedral symmetry. With successive replacement of alkaline earth content into glass matrix there is a small variation in g-values and it is shown in table 7, which indicates that ions that might be responsible for EPR lines broadening and participated in dipolar interaction. The hyperfine structure (hfs) is suitable to isolated Mn^{2+} ions in octahedral sites that are alienated well enough from each other to avoid strong dipolar interactions. g factor value and well-resolved hfs support this statement and also give evidence for the predominantly ionic character

of the bonding between Mn^{2+} and the O^{2-} ions generating the octahedral symmetric ligand field. From figure 5 it was concluded that resonance signal at $g \approx 2.0$ which is due to Mn^{2+} ion in an environment close to the octahedral symmetry.[35] EPR spectral studies reveal the nature of the bonding is dominantly ionic and its site symmetry is octahedral.

FTIR absorption spectra gives information about molecular vibrations as well as rotation associated with a covalent bond. Transmission spectra of all the phosphate glasses accumulated in the range 1400–400 cm^{-1}. The FTIR spectra are interpreted on the basis of the vibration of the phosphate glass structural units close to the subsequent crystalline

analogues.[36,37] FTIR spectra for present glass systems are shown in figure 6. Bands at 1280 and 1320 cm^{-1} is especially meaningful, as it is due to the anti-symmetrical vibrations of PO$_2^-$ groups/P=O stretching.[38] The band ~1200 cm^{-1} is consign to the symmetrical stretching vibrations (ν_s(O–P–O)) group of non-bridging oxygen in phosphate chain.[39] The band at 1180 cm^{-1} is due to the vibrations of PO$_3^{2-}$ groups at the end of chains.[40] The observed band at ~1080 cm^{-1} is assigned to a normal vibrational mode of PO$_4^{3-}$ group arising out of ν_3-symmetric stretching. The bands around 950–980 cm^{-1} are due to P–O–P asymmetric bending vibrations/this region may also consist of bands due to pyrophosphate groups P$_2$O$_7^{4-}$. An asymmetric stretching vibration ν_{as}(P–O–P) is observed at 910 cm^{-1} in the spectra is the characteristic of Q^1 group.[37] The bands at about 900–1100 cm^{-1} can be assigned to phosphate units with progressive replacement of alkali earth oxides from MgO to BaO.[41] Another band in the region of 760–780 cm^{-1} is due to P–O–P symmetric stretching vibrations. The band at 660 cm^{-1} is attributed to P–O–P. The band at about 700 cm^{-1} is ascribed to P–O–P symmetrical stretching vibration mode.[42] The vibrational modes observed at 530, 540 and 580 cm^{-1} for all the glasses are due to the bending mode of the phosphate polyhedra and/or Pb–O and Zn–O vibrations. The formation of these bonds replaces easily hydrolysable P–O–P bonds.[43] Some bands are shifted toward higher wavenumber, i.e., those corresponding to the P=O double bond, both

of symmetric and antisymmetric stretching P–O–P modes and harmonic bending mode of P–O–P bond. The effect of successive addition of alkaline earth is observed in the increase of the peak at 1080 cm^{-1} and the decrease of the peaks at 730 cm^{-1} which clearly indicate the increase of the pyrophosphate units on the expense of the decrease of the metaphosphate units. These activities can be due to the depolymerization process inside the glass network.[44] With successive substitution of MgO/CaO/SrO/BaO content, glass matrix leads to more P=O bonds breakage and to form P–O–Mg/P–O–Ca/P–O–Sr/P–O–Ba bonds.[45–48] Alkaline earth oxides enter the glass network interstitially, as a network modifier; and we know that when modifier cations are added to phosphate glasses depolymerization takes and formation of ionic cross bonding between phosphate chains.

The prevalence of any particular Q species is dependent on the metal oxide content of the glass composition. The addition of metal ions will make Q^n species present in the phosphate glass network.[49] In phosphate glasses with [P$_2$O$_5$] >50 mol%, the structural types of units are Q^3 and Q^2 tetrahedra.[50]

The changes of the Raman spectra with composition are used to deduce the structural evolution of the samples. The basic structural element of phosphate glass is the [PO$_4$] tetrahedron. The addition of modifying oxides leads to the scission of P–O–P bonds and to the network depolymerization.[51] The Raman spectra of the studied glasses are shown in

Table 6. Optical band gap (E_{opt}) and Urbach (ΔE) energies of Mn^{2+}-doped alkaline earth lead zinc phosphate glasses.

Samples	Optical band gap energy E_{opt} (eV)	Urbach energy ΔE (eV)
TG4A	3.458	0.256
TG4B	3.130	0.284
TG4C	3.174	0.232
TG4D	2.815	0.198

Table 7. Summary of the data on EPR of Mn^{2+}-doped alkaline earth lead zinc phosphate glasses.

Sample	g (signal 1)	g (signal 2)	A (10^{-4} cm^{-1})
TG4A	2.0285	4.2988	89.75
TG4B	2.0256	4.2988	89.62
TG4C	2.0244	4.2988	90.97
TG4D	2.0273	4.2988	89.99
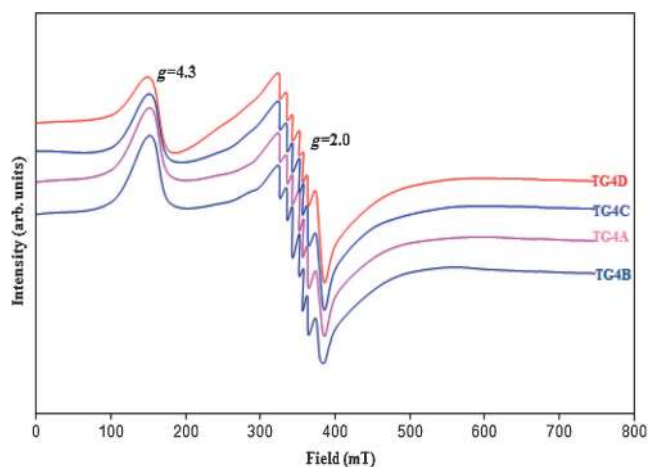
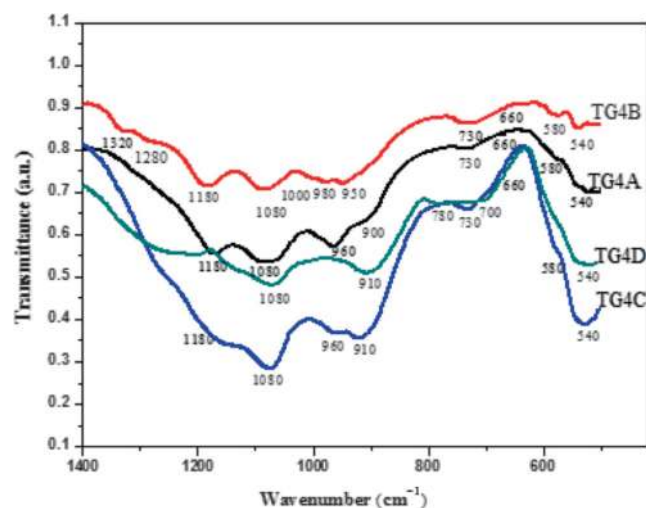**Figure 5.** EPR spectra of Mn^{2+}-doped alkaline earth lead zinc phosphate glasses.

Figure 6. FTIR spectra of Mn^{2+}-doped alkaline earth lead zinc phosphate glasses.
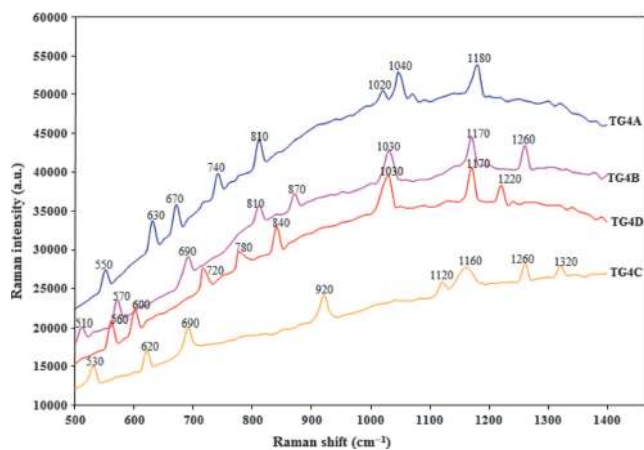
Figure 7. Raman spectra of Mn^{2+}-doped alkaline earth lead zinc phosphate glasses.

figure 7. The change in peak position of bands could be help to get more insight into the effect of alkaline earth on the phosphate network. On the basis of the assignments of Raman spectra for the present glasses, the bands at 1120–1170 cm^{-1} attributed to vibrations of PO$_2^-$ in Q^2 units, band 1320 cm^{-1} due to the P=O symmetric stretching vibrations.[52,53] The peaks between 1120 and 1140 cm^{-1} is elucidated by Q^2 groups interacting with different cations such as $Mg^{2+}/Ca^{2+}/Sr^{2+}/Ba^{2+}$.[54] Band at 1250 cm^{-1} is attributed to (PO$_2$)$_{as}$ stretch, Q^2 units.[55] The depolarized Raman band at about 1260 cm^{-1} is assigned to asymmetric stretching vibrations of the non-bridging oxygen's against P atoms. Band at around 800 and 1020–1040 cm^{-1} are related to the symmetric stretching mode of bridging (P–O–P) sym and non-bridging (PO$_2$)sym oxygen atoms in Q^1 phosphate terahedra,[56] band at 920 cm^{-1} assigned to vibration in PO$_2^-$ and PO$_3^-$ groups.[57] The band at 780 cm^{-1} is due to (P–O–P)$_s$ stretch in very short phosphate chains or in ring structure.[58] Band at $\sim$650 cm^{-1} due to the vibration of P–O–P in-chain, bands at about 670–690 cm^{-1} are assigned to the symmetric in-plane bending vibration, ν_s (P–O–P), of bridging oxygens connecting two PO$_4$ tetrahedra.[59] The bands at 550–580 cm^{-1} are a sign of the (O–P–O) bending in the Q^1 structure and/or Zn-O tetrahedral bonds indication.[60]

FTIR and Raman spectra of the studied glasses are influenced by the network modifiers as well as transition metal oxide. Depolymerization of phosphate chains in all the glasses is observed with replacement of alkaline earth content by spectroscopic studies. This leads to a strong decrease of the average chain length and a small decreasing of the average P–O–P bridging angle with replacement of alkaline earth content.

4. Conclusions

XRD diffractograms reveal the amorphous nature of manganese-doped alkaline earth lead zinc phosphate glasses. From optical absorption spectra of Mn^{2+} ions in glasses, it is concluded that the site symmetry of the Mn^{2+} ion is tetragonally distorted octahedral. Optical band gap energy and Urbach energy are found to be dependent upon variation of alkaline earth content. DSC results indicate that barium ions increase cross-link density and enhance mean bond strength in TG4D glass. EPR investigations indicated the presence of two signals: an isotropic one at $g = 2.0$ which is due to Mn^{2+} in an environment close to the octahedral symmetry and a very well absorption centred at $g = 4.3$ which is characteristic for isolated Mn^{2+} ions in cubic symmetric sites slightly tetragonally or rhombically distorted. From EPR and optical spectral studies reveals the nature of the bonding is dominantly ionic and its site symmetry is octahedral. The predominant phosphate units occurring in doped sampled glasses are noticed by Raman spectra and it is supported by FTIR spectra also. Vibrational spectral features indicate a depolymerization process of the phosphate network with successive substitution of alkaline earth content. This process implies an increase of the number of non-bridging oxygen.

References

1. Gautam C R, Kumar D, Parkash O and Singh P 2013 *Bull. Mater. Sci.* **36** 461
2. Motke S G, Yawale S P and Yawale S S 2002 *Bull. Mater. Sci.* **25** 75
3. Loong C K, Suzuya K, Price D L, Sales B C and Boatner L A 1997 *Physica B* **241–243** 890
4. Liu H S and Chin T S 1997 *Phys. Chem. Glasses* **38** 123
5. Keun Lee Y and Choi S H 2008 *J. Korean Acad. Periodontol.* **38** 273
6. Kreidl N J 1990 *J. Non-Cryst. Solids* **123** 337
7. Ravikumar R V S S N, Ikeda K, Chandrasekhar A V, Reddy Y P, Rao P S and Jun Y 2003 *J. Phys. Chem. Solids* **64** 2433
8. Osipov A A, Osipova L M and Eremyashev V E 2013 *Glass Phys. Chem.* **39** 105
9. Srinivasa Rao A, Rupa Venkateswara Rao B, Prasad M V V K S, Shanmukha Kumar J V, Jayasimhadri M, Rao J L and Chakradhar R P S 2009 *Physica B* **404** 3717
10. Weber M J, Saroyan R A and Ropp R C 1981 *J. Non-Cryst. Solids* **44** 137
11. Gaafar M S, Marzouk S Y and Mady H 2009 *Philos. Mag.* **89** 2213
12. Shelby J E 2005 *Introduction to glass science and technology* (Cambridge: Royal Society of Chemistry) 2nd ed
13. Sanjay S, Kishore N S and Agarwal A 2009 *J. Alloys Compd.* **487** 52
14. Saddeek Y B 2009 *J. Alloys Compd.* **467** 14

15. Duffy J A and Ingram M D 1975 *J. Inorg. Nucl. Chem.* **37** 1203

16. Hurby A 1972 *Czech. J. Phys. B* **22** 1187

17. Ray N H 1974 *J. Non-Cryst. Solids* **15** 423

18. Shelby J E 1983 *J. Am. Ceram. Soc.* **66** 225

19. Button D P, Tondon R, King C, Velez M H, Tuller H L and Uhlmann U R 1982 *J. Non-Cryst. Solids* **49** 129

20. Martin S W and Angell C A 1984 *J. Non-Cryst. Solids* **66** 429

21. Dummy R 1980 *J. Non-Cryst. Solids* **41** 273

22. Srinivasa Rao A, Sreedher B and Rao J L 1992 *J. Non-Cryst. Solids* **144** 169

23. Machado I E C, Prado L, Gomes L, Prison J M and Martinelli J R 2004 *J. Non-Cryst. Solids* **348** 113

24. Henderson B 2000 *Crystal-field engineering of solid-state 424 laser materials* (Cambridge: Cambridge Press)

25. Tanabe Y and Sugano S 1954 *J. Chem. Soc. Jpn.* **9** 753

26. Trees R E 1951 *Phys. Rev.* **83** 756

27. Burns R G 1993 *Mineralogical applications of crystal field theory* (Cambridge: Cambridge University Press)

28. Mort N F and Davis E A 1971 *Electronic processes in non-crystalline materials* (Oxford: Clarendon)

29. Urbach F 1953 *Phys. Rev.* **92** 1324

30. Tauc J and Abeles F 1970 *Optical properties of solids* (Berlin: Springer)

31. Abdel-Baki M, El-Diasty F and Wahab F A A 2006 *Opt. Commun.* **261** 65

32. Viviani D, Faivre F, Levelut C and Smaihi M 2006 *J. Phys. Chem. B* **110** 7281

33. Van Wieringen J S 1955 *Discuss. Faraday Soc.* **19** 118

34. Abragam A and Bleaney B 1970 *Electron paramagnetic resonance of transition ions* (Oxford: Clarendon)

35. Giridhar G, Rangacharyulu M, Ravikumar R V S S N and Sambasiva Rao P 2009 *IOP Conf. Ser.: Mater. Sci. Eng.* **2** 012058

36. Efimov A M 1996 *J. Non-Cryst. Solids* **203** 1

37. Montagne L, Palavit G and Mairesse G 1996 *Phys. Chem. Glasses* **37** 206

38. Elisa M *et al* 2010 *J. Optoelectron. Adv. Mater.* **4** 1301

39. Rohaizada A, Hussina R, Syaqilah Aziza N A, Uninga R and Boharia N Z I 2013 *Jurnal Teknologi* **62** 119

40. Le Saout G, Simon P, Fayon F, Blin A and Villas Y 2002 *J. Raman Spectrosc.* **33** 740

41. Yiannopoulos Y D, Chryssikos G D and Kamitsos E I 2001 *Phys. Chem. Glasses* **42** 164

42. El-Ahdal M A, Antar E M, Mahmoud H H and Ezz-Eldin F M 2011 *J. Appl. Sci. Res.* **7** 1434

43. Abid M, Elmoudane M and Et-tabirou M 2002 *Phys. Chem. Glasses* **43** 267

44. Metwalli E, Karabulut M, Sidebottom D L, Morsi M M and Brow R K 2004 *J. Non-Cryst. Solids* **344** 128

45. Peng Y B and Day D E 1984 *Glass Technol.* **5** 166

46. Hudgens J J and Martin S W 1994 *J. Am Ceram. Soc.* **76** 1691

47. Bunker B C, Arnold G W and Wilder J A 1984 *J. Non-Cryst. Solids* **64** 291

48. Ardelean I, Andronache C, Câmpean C and Pascuta P 2004 *Mod. Phys. Lett. B* **18** 45

49. Van Wazer J R 1958 *Phosphorous and its compounds* (New York: Inter-Science) vol. 1

50. Schwarz J, Tichá H, Tichýa L and Mertens R 2004 *J. Optoelectron. Adv. Mater.* **6** 734

51. Hoppe U 1996 *J. Non-Cryst. Solids* **195** 138

52. Hudgens J J, Brow R K, Tallant D R and Martin S W 1998 *J. Non-Cryst. Solids* **223** 21

53. Scagliotti M, Villa M and Chiodelli G 1987 *J. Non-Cryst. Solids* **93** 350

54. Brauer D S, Karpukhina N, Law R V and Hill R G 2010 *J. Non-Cryst. Solids* **356** 2626

55. Meyer K 1997 *J. Non-Cryst. Solids* **209** 227

56. Šantic A, Moguš-Milankovic A, Furic K, Bermanec V, Kim C W, and Day E 2007 *J. Non-Cryst.* **353** 1070

57. Garbarczyk J E, Machowski P, Wasiucionek M, Tykarski L, Bacewicz R and Aleksiejuk A 2000 *Sol. State Ionics* **136** 1077

58. Brow R K, Tallant D R, Warren W L, McIntyre A and Day D E 1997 *Phys. Chem. Glasses* **38** 300

59. Zotov N, Schlenz H, Brendebach B, Modrow H, Hormes J, Reinauer F, Glaum R, Kirfel A and Paulmann C 2003 *Z. Naturforsch.* **58**(a) 419

60. Magdas D A, Cozar O, Chis V, Ardelean I and Vedeanu N 2008 *Vib. Spectrosc.* **48** 251